Biochemistry

pubs.acs.org/biochemistry Article

Targeting a Pathogenic Cysteine Mutation: Discovery of a Specific Inhibitor of Y279C SHP2

Jenny Y. Kim, Bailey A. Plaman, and Anthony C. Bishop*

Cite This: *Biochemistry* 2020, 59, 3498–3507 Read Online

ACCESS | Metrics & More | Article Recommendations | Supporting Information

ABSTRACT: An intriguing challenge of drug discovery is targeting pathogenic mutant proteins that differ from their wild-type counterparts by only a single amino acid. In particular, pathogenic cysteine mutations afford promising opportunities for mutant-specific drug discovery, due to the unique reactivity of cysteine's sulfhydryl-containing side chain. Here we describe the first directed discovery effort targeting a pathogenic cysteine mutant of a protein tyrosine phosphatase (PTP), namely Y279C Src-homology-2-containing PTP 2 (SHP2), which has been causatively linked to the developmental disorder Noonan syndrome with multiple lentigines (NSML). Through a screen of commercially available compounds that contain cysteine-reactive functional groups, we have discovered a small-molecule inhibitor of Y279C SHP2 (compound **99**; $IC_{50} \approx 6\ \mu M$) that has no appreciable effect on the phosphatase activity of wild-type SHP2 or that of other homologous PTPs ($IC_{50} \gg 100\ \mu M$). Compound **99** exerts its specific inhibitory effect through irreversible engagement of Y279C SHP2's pathogenic cysteine residue in a manner that is time-dependent, is substrate-independent, and persists in the context of a complex proteome. To the best of our knowledge, **99** is the first specific ligand of a disease-causing PTP mutant to be identified. This study therefore provides both a starting point for the development of NSML-directed therapeutic agents and a precedent for the identification of mutant-specific inhibitors of other pathogenic PTP mutants.

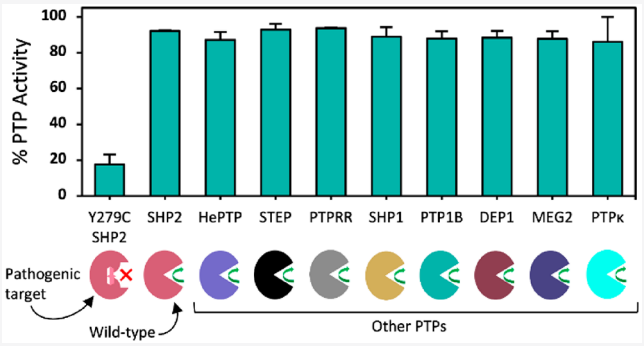

It has long been recognized that the nucleophilic reactivity of cysteine's sulfhydryl group provides a potent handle for the development of electrophilic small-molecule covalent inhibitors.[1−3] When a therapeutic target is a member of a large protein family, however, not all of its cysteine residues hold equal potential as sites for drug discovery. Cysteines that are highly conserved among a protein family do not suggest clear strategies for achieving selectivity between members of the family. By contrast, nonconserved cysteines can provide a means for the development of selective inhibitors, and such "rare" cysteine residues have previously been targeted to achieve selective inhibition in a number of protein families, most notably the protein kinases.[4−6] Further opportunities for targeting nonconserved cysteines in drug discovery can be found in cases of disease-causing missense mutations; when a cysteine mutation is itself pathogenic, the causative agent presents a potentially targetable molecular handle that can be differentiated from both the wild-type protein and its homologues.[7] Recent work on the oncogenic KRAS(G12C) mutant has provided a remarkable demonstration of the potential impact of targeting pathogenic cysteine mutations and has led to the development of AMG510, the first KRAS(G12C) inhibitor to reach clinical trials.[8−10] These seminal findings suggest a follow-up question. Are there disease-causing cysteine mutations in other protein families that could be potentially targeted for the development of mutant-selective therapeutic agents? Indeed, a cysteine mutant (Y279C) of Src-homology-2-containing protein tyrosine phosphatase 2 (SHP2), which is the focus of this study, has been identified as a causative agent of Noonan syndrome with multiple lentigines (NSML, formerly called LEOPARD syndrome).[11−14]

SHP2 is a member of the protein tyrosine phosphatase (PTP) family, a critical set of cell-signaling enzymes that catalyze the removal of phosphate groups from phosphotyrosine residues. SHP2, a ubiquitously expressed PTP, plays key roles in the control of signaling events involved in cell growth and proliferation, such as the Ras/MAPK and PI3K/AKT pathways.[14−16] SHP2's PTP activity in these pathways is controlled by an autoinhibitory interaction between the enzyme's catalytic (PTP) domain and its amino-terminal SH2 domain (N-SH2), in which the N-SH2 domain blocks the

Received: June 3, 2020
Revised: August 31, 2020
Published: September 1, 2020

https://dx.doi.org/10.1021/acs.biochem.0c00471
Biochemistry 2020, 59, 3498–3507

PTP domain's active site.[17−19] SHP2 is transiently activated in a cell-signaling pathway when its N-SH2 engages a phosphorylated protein target, causing a conformational change that releases the PTP domain from autoinhibition.[17−19] Mutations that alter the inherent strength of SHP2's autoinhibitory interaction lead to misregulation of its activity and are causative agents of both cancers and developmental disorders.[11] The intimate connection between inappropriately regulated SHP2 activity and pathogenesis makes the enzyme an appealing drug target, and compounds that bind to and stabilize SHP2's autoinhibited conformation have demonstrated considerable promise as anticancer therapeutics.[20,21] However, no small molecules that specifically target disease-associated SHP2 mutants have been previously identified.

Missense mutations in SHP2 are causative agents for the developmental disorders Noonan syndrome and NSML, which are both characterized by reduced growth, abnormalities in facial structure, congenital heart defects, skeletal anomalies, and cognitive deficits.[11−14,22,23] Paradoxically, given the overlapping symptomatology between the two disorders, Noonan-causing SHP2 mutations generally increase SHP2's activity, whereas NSML-causing mutations reduce its *in vitro* enzymatic activity. The PTP domain of one of the most common NSML-causing SHP2 variants contains a cysteine mutation (Y279C) that substantially reduces the catalytic domain's intrinsic activity (wild-type SHP2 k_{cat} = 6.5 s^{-1}; Y279C SHP2 k_{cat} = 0.56 s^{-1}, with *p*-nitrophenyl phosphate as the substrate)[24] by disrupting key interactions between the Y279 side chain (in the wild-type protein) and phosphotyrosine-containing substrates.[13,24,25] More subtly, the autoinhibitory N-SH2/PTP-domain interaction is also weakened in the mutant, as an important interdomain interaction between residue 279 and Y62 of the N-SH2 domain is attenuated by the Y279C mutation (Figure S1).[13,25] Due to the weakened autoinhibition, downstream SHP2-mediated signaling events, such as phosphorylation of the key signaling molecule ERK, can, in some instances, be upregulated in Y279C SHP2-expressing cells, despite the lower inherent activity of the enzyme's catalytic domain.[13,24−27] Importantly, these signaling events are dependent on Y279C's residual SHP2 catalytic activity, as expression of Y279C/catalytic-dead double mutants does not lead to an increased level of signaling.[13,24−26] These findings help to resolve the paradox of a reduced-activity NSML mutant that presents a phenotype akin to those of gain-of-function mutants: attenuated autoinhibition in Y279C SHP2 can lead to heightened downstream signaling in a cellular context, despite the protein's low *in vitro* activity.

Compounds that reduce hypertrophic cardiomyopathy in a Y279C-SHP2-expressing NSML mouse model have been previously identified.[28,29] These compounds, however, act downstream of Y279C SHP2 and are not direct ligands of the causative mutant. The goal of this study is the identification of compounds that directly target Y279C SHP2 activity. Two different strategies toward this goal could be envisioned, given the counterintuitive enhanced-signaling phenotype that can derive from the activity-reducing Y279C mutation. In principle, one could attempt to identify Y279C SHP2 activators that engage C279 and restore wild-type-like enzymatic activity by filling the "hole" left by the tyrosine-to-cysteine mutation. Alternatively, compounds that specifically engage the pathogenic cysteine residue and inhibit Y279C SHP2's PTP activity could represent promising leads for treatment of NSML. Such compounds would, in effect, recapitulate the Y279C/catalytic-dead double mutant phenotype; blocking the pathogenic mutant's residual activity would presumably also block the aberrant downstream signaling events caused by its activity.

In this study, we identify and characterize compound **99**, a specific inhibitor of Y279C SHP2. The compound directly engages Y279C SHP2's NSML-causing cysteine residue and blocks the activity of the mutant enzyme, while demonstrating no measurable inhibitory activity against wild-type SHP2 and other homologous PTP enzymes. To the best of our knowledge, **99** is the first specific ligand of Y279C SHP2 and therefore represents a starting point for the development of NSML-directed therapeutic agents. In broader terms, the screening strategy employed to identify **99** provides a potential blueprint for the identification of mutant-specific ligands of other disease-associated SHP2 mutants.

MATERIALS AND METHODS

General and Materials. "% PTP activity" is defined as the initial velocity of phosphatase activity in the presence of compound **99** divided by the initial velocity of phosphatase activity in a vehicle-only (DMSO) control. The data presented are an average ± the standard deviation of three independent data points, with the exception of the initial compound-library screen, which was carried out with single-point assays. Compounds screened were purchased from Life Chemicals as a part of their Cysteine Reactive Compound Library and used without further purification. Additional **99** was purchased from Life Chemicals and Princeton Biomolecular Research, Inc., and used without further purification.

PTP-Encoding Plasmid Vectors. The pET vectors encoding His_6-tagged catalytic domains (CDs) of wild-type human SHP2 (pDK012; UniProtKB Q06124, amino acids 224−539), PTP1B (pOBD002l; UniProtKB P18031, amino acids 1−295), HePTP (pET-HePTP-6his; UniProtKB P35236, amino acids 65−360), PTPRR (pBAP004; UniProtKB Q15256, amino acids 373−657), SHP1 (pACB149; UniProtKB P29350, amino acids 243−541), and PTPκ (pDK002; UniProtKB Q15262, amino acids 870−1154) have been previously described.[30−32] The pET vector encoding His_6-tagged full-length SHP2 (pAC005; UniProtKB Q06124, amino acids 1−541) has also been previously described.[32] The pET vectors encoding the His_6-tagged catalytic domains of STEP (pDK016; UniProtKB P54829, amino acids 282−565), DEP1 (pDK003; UniProtKB Q12913, amino acids 1024−1316), and MEG2 (pDK004; UniProtKB P43378, amino acids 286−592) were purchased from VectorBuilder. Plasmids for the expression of the His_6-tagged Y279S SHP2 CD (pJYK005) and His_6-tagged Y279C SHP2 CD (pJYK003) and full-length (pJYK001) mutants were generated via the QuikChange II site-directed mutagenesis kit (Agilent), and desired mutations were confirmed via DNA sequencing by the Cornell Biotechnology Resource Center.

Protein Expression and Purification. All PTPs were expressed as previously described and purified using HisPur Ni-NTA resin per the manufacturer's instructions.[32] Purified PTPs were exchanged into storage buffer [50 mM 3,3-dimethylglutarate (pH 7.0) and 1 mM EDTA, supplemented with 1 mM TCEP], concentrated, flash-frozen with liquid nitrogen, and stored at −80 °C. The protein concentration was determined using a NanoDrop spectrophotometer, and the

https://dx.doi.org/10.1021/acs.biochem.0c00471
Biochemistry 2020, 59, 3498−3507

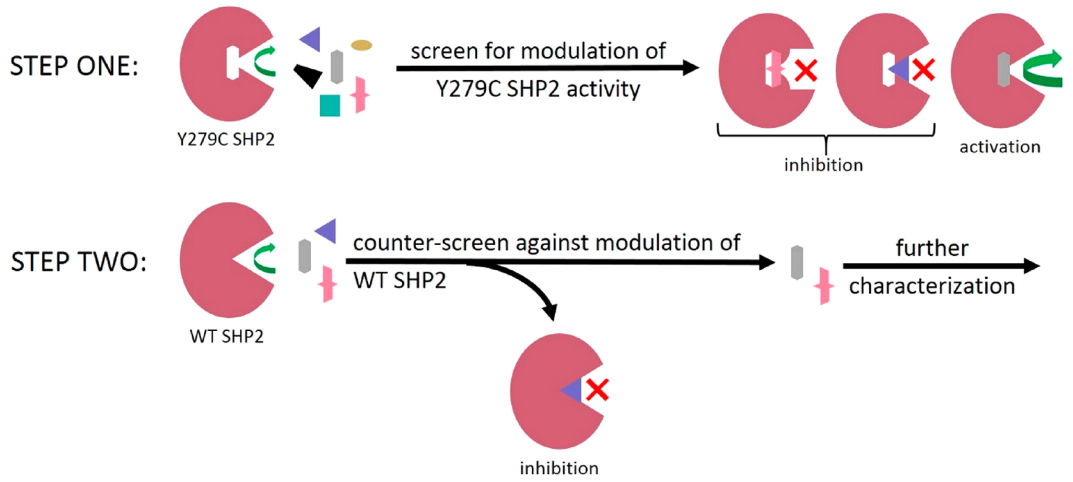

Figure 1. Screen for specific modulators of Y279C SHP2 activity. Compounds from the Life Chemicals Cysteine Reactive Compound Library were screened on the basis of changes in Y279C SHP2 phosphatase activity relative to a vehicle-only control. Compounds that inhibited Y279C SHP2 to <30% activity (pink and purple compounds) or activated Y279C SHP2 to >100% activity (gray compound) were subjected to a subsequent counterscreen against wild-type SHP2 to ensure Y279C-specific modulation. In this example, the purple compound is an active site-directed inhibitor of both Y279C and wild-type SHP2. Thus, only gray and pink compounds would be selected for further characterization.

purity was assessed by sodium dodecyl sulfate−polyacrylamide gel electrophoresis.

Phosphatase Activity Assays with DiFMUP. Phosphatase activity was monitored by the rate of dephosphorylation of 6,8-difluoro-4-methylumbelliferyl phosphate (DiFMUP) as indicated by increasing emission at 455 nm. Reactions were carried out in a total volume of 200 μL of PTP buffer 1 [25 mM MOPS (pH 7.0), 50 mM sodium chloride, and 0.05% Tween 20] supplemented with 1 mM DTT and 0.004 mg/mL BSA with enzyme, compound or vehicle, and DiFMUP. All experiments were carried out at 2% (v/v) DMSO unless otherwise indicated. See the figures for concentrations and preincubation conditions.

Compound Screening. Compounds were purchased as DMSO stock solutions (10 mM). Compounds were diluted in DMSO (1 mM) and added to screens at a final concentration of 10 μM. Reactions were carried out in a total volume of 200 μL of PTP buffer 1 (see above) supplemented with 1 mM DTT and 0.004 mg/mL BSA with Y279C SHP2 CD (75 nM). Reaction mixtures were incubated with a compound at 37 °C for 1 h before phosphatase activity was assayed at 1.5% (v/v) DMSO with 40 μM DiFMUP essentially as outlined above. Compounds that inhibited (<30% PTP activity) or activated (>120% PTP activity) Y279C SHP2 CD were performed in triplicate before counterscreening against wild-type SHP2 CD (12.5 nM) under the same reaction conditions.

Differential Scanning Fluorimetry. To determine the melting temperatures of wild-type and Y279C SHP2 CD, protein samples consisting of SHP2 CD (10 μM WT and 15 μM Y279C) and SYPRO Orange Protein Gel Stain (Thermo Scientific, 25×) in DSF buffer [20 mM HEPES (pH 7.5), 50 mM sodium chloride, and 1 mM TCEP] for a total volume of 25 μL were subjected to a change in temperature at a rate of 1.0 °C/min from 25.0 to 95.0 °C on a RT-PCR machine. The fluorescence of SYPRO Orange (excitation, FAM filter; emission, ROX filter) in each protein sample was recorded every 0.5 °C, and the inflection point of the resulting curve was taken as the melting temperature of the protein.

Phosphatase Activity Assays with a Phosphopeptide Substrate. Phosphatase activity was monitored by the dephosphorylation of phosphopeptide DADEpYLIPQQC as indicated by increasing the absorbance at 282 nm, essentially as described previously.[33] After a 1 h incubation at 37 °C in PTP buffer 2 [50 mM 3,3-dimethylglutarate (pH 7.0), 1 mM EDTA, and 50 mM sodium chloride] with SHP2 [varying concentrations (see the figures)] and **99** (37.5 μM) or vehicle at a final DMSO concentration of 1% (v/v), reactions were started upon addition of the phosphopeptide (100 μM) and carried out in a total volume of 180 μL.

Reversibility Assay. SHP2 was incubated with **99** at 2% (v/v) DMSO in PTP buffer 2 (see above) for 1 h at 37 °C. Phosphatase activity of a dilution of the incubation mixture was assayed with DiFMUP as outlined above. The remaining incubation mixture was mixed with an equal volume of wash buffer [50 mM Tris-HCl (pH 8.0), 500 mM sodium chloride, and 50 mM imidazole] and bound to 50 μL of prewashed HisPur Ni-NTA resin for 30 min spinning at 4 °C. The beads were washed with wash buffer three times and eluted with elution buffer [50 mM Tris-HCl (pH 8.0), 500 mM sodium chloride, and 250 mM imidazole]. Phosphatase activity of the washed protein was assayed with DiFMUP as outlined above, and activities were normalized to the protein concentrations of the samples.

Liquid Chromatography Electrospray Ionization Mass Spectrometry (LC-MS). Samples were prepared essentially as described for the reversibility assay, except samples of 100 μM SHP2 with 120 μM **99** or vehicle-only (DMSO) were incubated in PTP buffer 1 (see above) supplemented with 1 mM DTT at 4% (v/v) DMSO before washing. After washing, LC-MS analysis was performed at the University of Massachusetts Amherst Mass Spectrometry Core Facility. Protein samples were diluted in a 1:1 ratio with 0.2% formic acid, and 10 μg of protein was injected onto an Acquity Protein BEH C4 column (300 Å, 1.7 mm, 2.1 mm × 50 mm; Waters, Milford, MA) connected to an Agilent 1100 HPLC system. The mobile phases were (A) 0.1% formic acid and (B) 0.1% formic acid in 99% acetonitrile. The system was equilibrated in 30% B at a flow rate of 150 μL/min, and the following gradient was applied following sample injection: 30% B for 1 min, 30% to 75% B over 5 min, 75% to 90% B over 1

https://dx.doi.org/10.1021/acs.biochem.0c00471
Biochemistry 2020, 59, 3498−3507

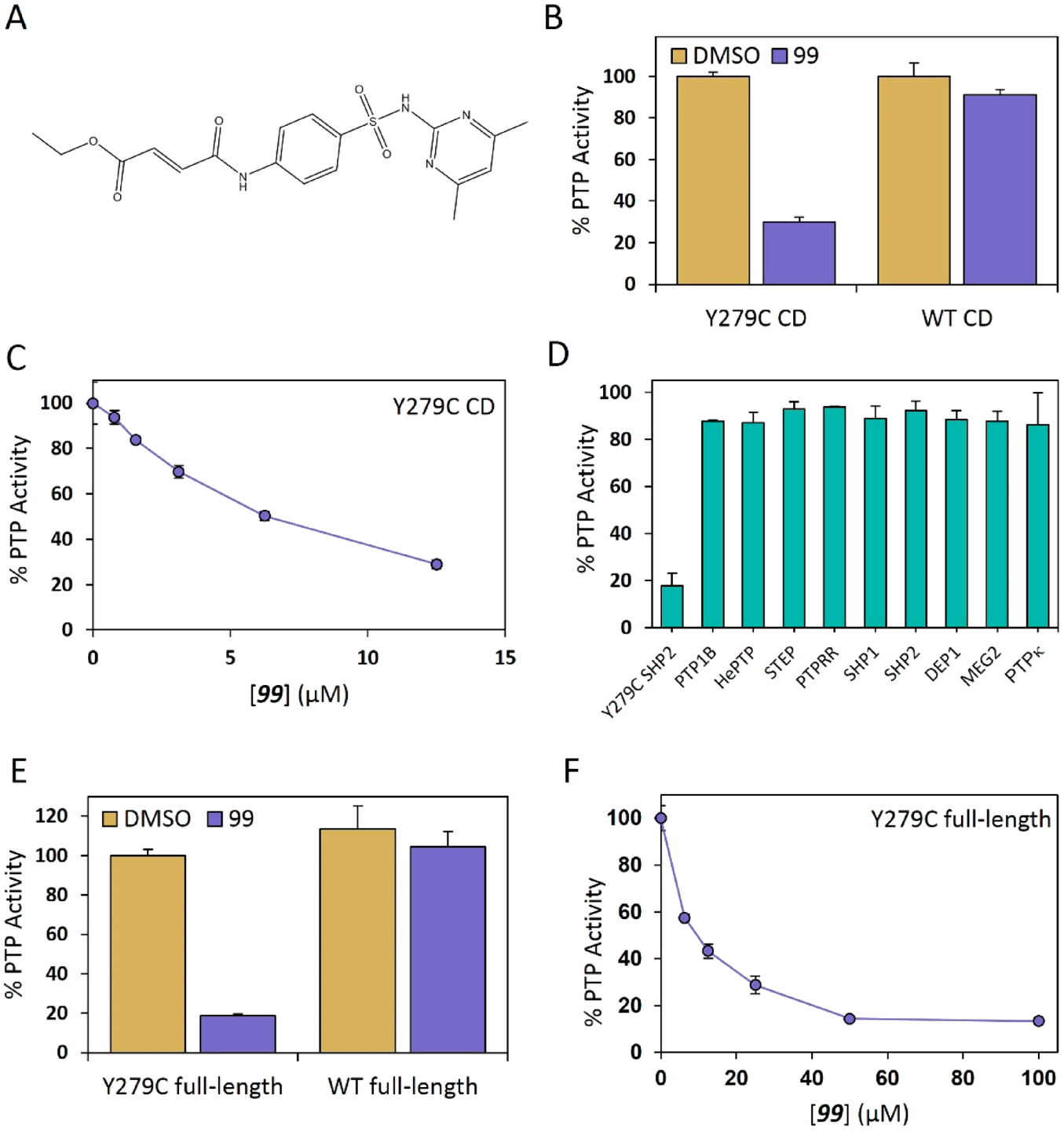

Figure 2. Compound **99** is a specific inhibitor of Y279C SHP2. (A) Chemical structure of compound **99**. (B) **99** inhibits the PTP activity of Y279C SHP2 CD but not wild-type SHP2 CD. SHP2 CD (100 nM) was incubated in the presence of 10 μM **99** (purple) or vehicle only (yellow) for 1 h at 37 °C. The PTP activity of Y279C (100 nM) and wild-type (16.7 nM) SHP2 CD was subsequently measured with 40 μM DiFMUP. (C) **99**-mediated inhibition of Y279C SHP2 CD is dose-dependent. PTP activity of 100 nM Y279C SHP2 CD was measured with 40 μM DiFMUP in the absence (DMSO) or presence of the indicated concentrations of **99** after a 1 h preincubation at 37 °C. (D) Compound **99** is highly selective for Y279C SHP2. Activities of the indicated PTP domains (100 nM Y279C SHP2, 100 nM STEP, 16.7 nM SHP2, 1 nM DEP1, and 1 nM PTPκ; all others at 25 nM) were measured with 40 μM DiFMUP in the absence (DMSO) or presence of 100 μM **99** after a 1 h preincubation at 37 °C. (E) **99** inhibits the PTP activity of full-length Y279C SHP2 but not full-length wild-type SHP2. Full-length Y279C (100 nM) and wild-type (12.5 nM) SHP2 were incubated in the presence of the activating peptide BTAM[36] (Y279C, 200 nM; wild type, 50 nM) and in the presence of 100 μM **99** (purple) or vehicle only (yellow) for 1 h at 37 °C. PTP activity was measured with 40 μM DiFMUP. (F) **99**-mediated inhibition of full-length Y279C SHP2 is dose-dependent. PTP activity of 50 nM full-length Y279C SHP2 in the presence of 200 nM BTAM was measured with 40 μM DiFMUP in the absence (DMSO) or presence of the indicated concentrations of **99** after a 1 h preincubation at 37 °C.

https://dx.doi.org/10.1021/acs.biochem.0c00471
Biochemistry 2020, 59, 3498−3507

min, and 90% B for 2 min. The flow was infused into a 7 T solariX FTICR mass spectrometer (Bruker, Billerica, MA) equipped with a standard electrospray source. The capillary voltage was 4.5 kV, the dry gas flow 8 L/min, and the dry gas temperature 200 °C. MS spectra were acquired over the range of m/z 300−3000 with a 128 K transient size and a 0.2 s accumulation time. Data were processed using DataAnalysis version 5.0 (Bruker).

Phosphatase Activity in SHP2-Expressing *Escherichia coli* Lysates. SHP2-expressing cell pellets were resuspended in PTP buffer 2 (see above) supplemented with 1 mM GSH and lysed via sonication. Clarified lysates were incubated at a total protein concentration of 1.175 mg/mL with **99** or DMSO for 1 h at 37 °C. Phosphatase activity of Y279C SHP2 was assayed with 50 μM DiFMUP essentially as described above. Because wild-type SHP2 CD activity is inherently higher than that of the mutant, the less sensitive substrate *p*-nitrophenyl phosphate (*p*NPP) was used to assay wild-type SHP2 CD. Reactions were carried out in a total volume of 200 μL and started upon addition of 1.5 mM *p*NPP. Reactions were quenched with 40 μL of 5 M sodium hydroxide, and the concentration of the dephosphorylated product (*p*-nitrophenolate) was determined by absorbance at 405 nm.

RESULTS AND DISCUSSION

Identification of a Y279C SHP2-Specific Inhibitor. To potentially identify compounds that can target the pathogenic cysteine residue of Y279C SHP2, we obtained a cysteine-reactive compound library, consisting of screening quantities of 200 small molecules (as DMSO solutions) that each contain an electrophilic moiety and a binding scaffold (Figure S2). The 200 compounds were screened for any modulation of Y279C SHP2's phosphatase activity as compared to a DMSO-only control (Figure S3), and compounds that strongly affected Y279C SHP2 activity were counterscreened against wild-type SHP2 (Figure 1). (The isolated catalytic domains of wild-type and Y279C SHP2 were used for the compound screen and many subsequent compound characterization experiments, as full-length SHP2 constructs have intrinsically low catalytic activity, because of autoinhibition by the enzyme's SH2 domains.)

One candidate compound emerged from our screen as a putative inhibitor of Y279C SHP2 [compound **99** (Figure 2A)]. At the screening concentration of 10 μM, the DMSO solution corresponding to compound **99** strongly inhibited the activity of the Y279C SHP2 catalytic domain (CD) but showed essentially no inhibition in a subsequent counterscreen against wild-type SHP2 CD (Figure 2B). (No Y279C SHP2 activators were identified in the compound screen.) To ensure that the active component of the DMSO solution that emerged from the screen has the presumed structure of **99**, we procured authentic **99** and confirmed its structure by nuclear magnetic resonance (NMR) and high-resolution mass spectrometry (Figure S4). Promisingly, **99**'s fumarate ester warhead has previously been used to target specific cysteine residues in other (non-PTP) medicinally important enzyme families.[34,35] It has also been shown that the fumarate ester's metabolic lability (i.e., susceptibility to hydrolysis by cellular esterases) can increase an inhibitor's target selectivity in a cellular context by reducing levels of slow, off-target cysteine engagement over long incubation times.[34]

To determine the potency of Y279C SHP2 CD inhibition by **99**, we incubated the enzyme with varying compound concentrations and determined the activities of the resulting solutions. Y279C SHP2 CD was inhibited in a dose-dependent manner with a 50% inhibitory concentration (IC_{50}) of ∼6 μM (Figure 2C). Out of concern that the Y279C mutation may destabilize the fold of the SHP2 catalytic domain fold and make it more prone to potential nonspecific aggregation by **99**, we determined the denaturing temperatures of both wild-type and Y279C SHP2 CD by differential scanning fluorimetry.[37] To our surprise, we found that the fold of Y279C SHP2 CD is more stable than that of the wild type, as demonstrated by a denaturing temperature that is approximately 6 °C higher for the mutant protein (Figure S5). It is unlikely that the more stably folded Y279C SHP2 CD would be more prone to chemically induced aggregation than the less stable wild-type protein.[38] Nevertheless, to further investigate the possibility that **99** induces nonspecific aggregation, we measured the potency of **99** in the presence of the detergent Triton X-100, which generally reduces the apparent inhibitory potency of nonspecific aggregators.[39,40] We found that the presence of Triton X-100 had no effect on **99**-mediated Y279C SHP2 CD inhibition (Figure S6), providing further evidence that **99** does not inhibit Y279C SHP2 CD's activity through nonspecific aggregation.

We next sought to more fully characterize the selectivity of **99** for Y279C SHP2 CD over other PTPs. Many catalytic domain-directed PTP inhibitors demonstrate only modest selectivity between PTPs, due to structural homology within the enzyme family.[15,41,42] However, no wild-type PTP has a cysteine residue at the position corresponding to 279 of SHP2 (Figure S7, human SHP2 numbering).[43] Therefore, if the presence of cysteine at position 279 is a strong determinant for **99**-mediated inhibition of Y279C SHP2, then one would expect **99** to show Y279C selectivity not only over wild-type SHP2 [as demonstrated by the initial compound screen (Figure 2B)] but also against other PTP family members. To test this hypothesis, we established a panel of nine PTP domains from six different PTP subfamilies[43] and measured their activities in the presence of a high concentration of **99** (100 μM). Consistent with the hypothesis that cysteine 279 is the critical determinant for Y279C SHP2 inhibition by **99**, we found that no members of the wild-type PTP panel were significantly inhibited by the compound, even at a concentration approximately 15-fold higher than **99**'s IC_{50} for Y279C SHP2 CD (Figure 2D).

Importantly, the specificity of compound **99** for Y279C SHP2 over wild-type PTPs remains operative in the context of a construct that contains the enzyme's regulatory SH2 domains (full-length). We found that the activity of full-length wild-type SHP2 is not affected by **99** (Figure 2E), whereas full-length Y279C SHP2 activity is inhibited in a dose-dependent manner (Figure 2F), with potency comparable to that observed with Y279C SHP2 CD ($IC_{50} \approx 10$ μM). Taken together, the data described above suggest that compound **99** is a specific inhibitor of Y279C SHP2 and, as such, represents the first known mutant-specific ligand for a pathogenic SHP2 variant.

Characterization of Y279C SHP2 Inhibition by Compound 99. The initial characterization of **99**'s ability to selectively inhibit Y279C SHP2 was carried out with an artificial small-molecule PTP substrate, 6,8-difluoro-4-methylumbelliferyl phosphate (DiFMUP) (Figure 2B−F). The cellular substrates of SHP2, however, are not small molecules; they are phosphorylated proteins. To potentially represent a useful ligand for targeting cellular Y279C SHP2, **99** must be

https://dx.doi.org/10.1021/acs.biochem.0c00471
Biochemistry 2020, 59, 3498−3507

capable of blocking the mutant's activity on phosphoproteins, and it must do so regardless of the substrate(s) encountered under particular cellular conditions. To test the substrate independence of Y279C SHP2 inhibition by **99**, as well as the ability of the compound to inhibit its target with a substrate that is more physiologically relevant than DiFMUP, we measured Y279C SHP2 CD activity on a phosphopeptide derived from an autophosphorylation site on the epidermal growth factor receptor (DADEpYLIPQQG)[44] in the absence and presence of **99**. Consistent with the previous observations using DiFMUP as the substrate, we found that the presence of **99** strongly inhibited Y279C SHP2 CD's dephosphorylation of DADEpYLIPQQG (Figure 3A) but had no inhibitory effect on

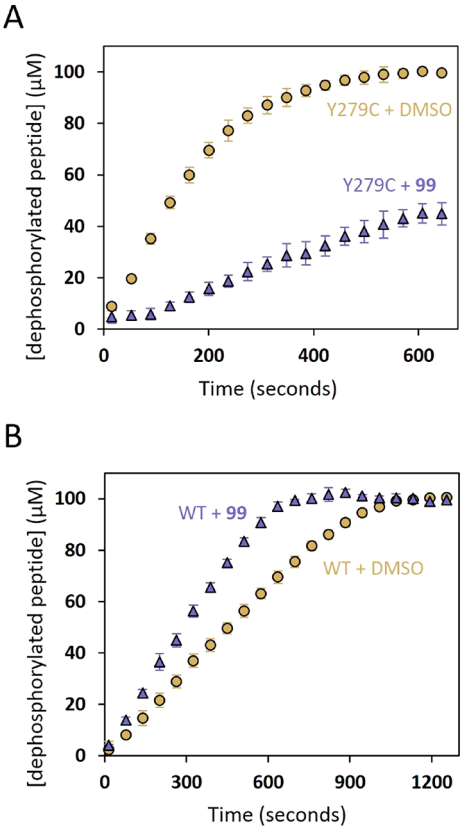

Figure 3. 99-mediated inhibition of Y279C SHP2 is independent of the substrate. (A) The activity of 2 μM Y279C SHP2 CD was measured with the phosphopeptide DADEpYLIPQQG (100 μM) as a substrate in the absence (DMSO, yellow circles) or presence of 37.5 μM **99** (purple triangles) after preincubation for 1 h at 37 °C. (B) The activity of 50 nM wild-type SHP2 CD was measured with the phosphopeptide DADEpYLIPQQG (100 μM) as a substrate in the absence (DMSO, yellow circles) or presence of 37.5 μM **99** (purple triangles) after preincubation for 1 h at 37 °C.

the ability of wild-type SHP2 CD to dephosphorylate the same peptide (Figure 3B). Curiously, addition of **99** appeared to induce a slight activation of wild-type SHP2 CD in the peptide dephosphorylation assay (Figure 3B). We cannot offer a strong hypothesis for the cause of this apparent increase in PTP activity, but we believe it is an artifact of the assay, as no significant activation was observed in other experiments in which wild-type SHP2 was treated with **99**.

To further probe the nature of **99**-mediated inhibition, we compared the kinetic parameters of **99**-treated Y279C SHP2 CD with those of the vehicle-treated enzyme. Michaelis–Menten kinetic analysis of Y279C SHP2 CD activity revealed a mixed mode of inhibition, as treatment with **99** (20 μM) induced both a 2-fold reduction in k_{cat} and a small increase in K_m relative to those of a DMSO-only control (Table 1 and

Table 1. Kinetic Constants of Y279C SHP2 CD Treated with DMSO or 99 (20 μM) and Assayed with DiFMUP

	k_{cat} (s^{-1})	K_M (μM)	k_{cat}/K_M (μM^{-1} s^{-1})
Y279C SHP2 with DMSO	7.7 ± 0.1	232 ± 9	0.033 ± 0.001
Y279C SHP2 with **99**	4.8 ± 0.1	340 ± 20	0.0141 ± 0.0009

Figure S8). These data are consistent with a model in which **99** binds at the site of C279, which lies close to the active site (Figure S1). Given the location of C279, it is plausible that binding of **99** could both lower the inherent activity of the enzyme and partially block substrate binding.

We next investigated the time dependence of **99**'s inhibitory action on Y279C SHP2 CD, and we found that the potency of inhibition is strongly time-dependent (Figure 4A). A quantitative analysis of the time and concentration dependence of **99**-mediated Y279C SHP2 CD inhibition revealed an inactivation rate (k_{inact}) of 0.0016 min^{-1}, and maximal inhibition at ∼20% activity (Figure 4). It is interesting that the maximal level of 80% inhibition was observed even at high compound concentrations and/or long incubation times (Figure 4A). This observation suggests that either the fully labeled protein retains approximately 20% of its activity or some structural factor of the protein precludes complete labeling (e.g., partial oxidation of the C279 side chain). Although time-dependent inhibition is not dispositive evidence of a covalent mode of inhibition, these data are suggestive that **99** exerts its inhibitory action through a relatively slow process, consistent with a covalent reaction between the mutant enzyme's C279 and the electrophilic inhibitor. We next sought more definitive evidence of C279 engagement by **99**.

Compound 99-Mediated Inhibition Is Covalent and Irreversible. To more fully test the hypothesis that **99** inhibits Y279C SHP2 through direct, covalent engagement of C279, we designed a series of experiments to probe key aspects of cysteine-directed inhibition. We first asked whether Y279C SHP2 inhibition by **99** is strictly dependent on the presence of cysteine at position 279. The mutation from tyrosine (wild-type SHP2) to cysteine (Y279C) is structurally non-conservative, and one could surmise that the mutation might have a range of effects on the protein's stability and/or inhibitor sensitivity [e.g., we showed previously that the mutation gives rise to a rather sizable stabilization of the catalytic domain's fold (Figure S5)]. However, if the mutant's sensitivity to **99** is strictly dependent on the unique nucleophilicity of cysteine, we would expect that the corresponding serine mutant (Y279S SHP2 CD, which differs by only a single atom in the position 279 side chain) would not be sensitive to inhibition by **99**. To determine if **99**'s inhibition of Y279C SHP2 CD is strictly dependent on the presence of C279, we measured the effect of **99** on Y279S SHP2 CD. We found that compound **99** exerted no substantial inhibitory effect on Y279S SHP2 CD, even at a concentration (100 μM) that far exceeds the compound's IC_{50} for Y279C SHP2 CD (Figure 5A). These findings suggest that the sulfur atom of the C279 side chain, and its attendant nucleophilicity, is required

https://dx.doi.org/10.1021/acs.biochem.0c00471
Biochemistry 2020, 59, 3498−3507

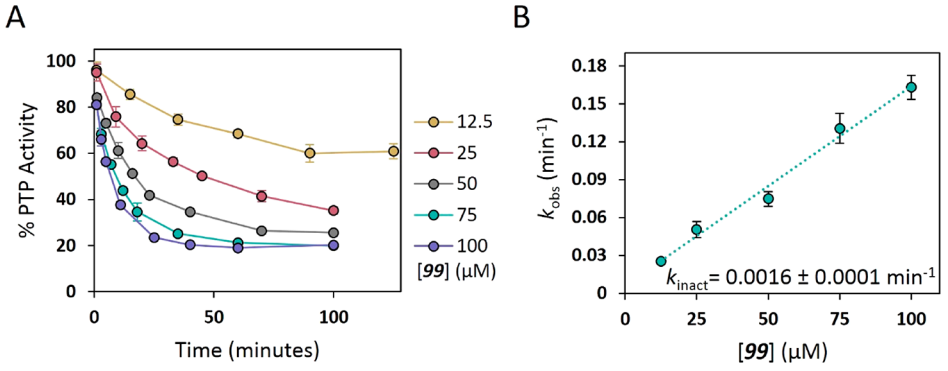

Figure 4. Kinetic analysis of SHP2 inhibition by **99**. (A) Time-dependent inhibition assays were carried out essentially as described in the legend of Figure 2B to determine the observed rate of inhibition (k_{obs}) at various concentrations of **99** (12.5 μM in yellow, 25 μM in pink, 50 μM in gray, 75 μM in turquoise, and 100 μM in purple). (B) k_{obs} was determined via curve fitting, and the linear relationship between k_{obs} and the inhibitor concentration was analyzed to estimate the indicated kinetic constant as previously described.[45,46]

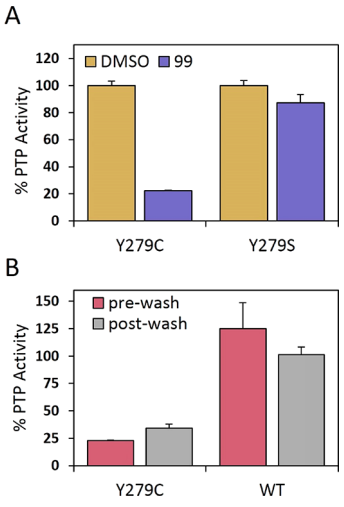

Figure 5. Compound **99**-mediated inhibition is covalent and irreversible. (A) **99**-mediated inhibition is covalent. PTP activity of 400 nM Y279C and Y279S SHP2 CD was measured with 40 μM DiFMUP in the absence (DMSO, yellow) or presence of 100 μM **99** (purple) after a 1 h preincubation at 37 °C. (B) **99**-mediated inhibition is irreversible. Twenty-five micromolar of SHP2 was incubated with 60 μM **99** for 1 h at 37 °C. The activity of Y279C and wild-type SHP2 was measured with 40 μM DiFMUP before (pink) and after (gray) washing out unbound **99**.

to render the SHP2 catalytic domain sensitive to inhibition by **99**.

We next sought to determine whether C279 engagement by **99** was reversible or irreversible by measuring the persistence of inhibition after removal of the compound. In this experiment, the phosphatase activity of six-histidine-tagged **99**-treated Y279C SHP2 CD was measured both before incubation with Ni-NTA beads and after copious washing of the Ni-NTA-immobilized enzyme. We found that strong inhibition of Y279C SHP2 CD activity by **99** persisted after washing away excess compound and subsequent elution of the enzyme from the beads (Figure 5B). The results show that the off rate of **99** binding to Y279C SHP2 is exceedingly low and suggest that **99** acts irreversibly on its target enzyme. In addition, the irreversibility of **99** is consistent with a model in which the compound covalently engages C279.

We next sought to confirm direct target engagement of C279 by mass spectrometry (MS). Generally, the tool of choice for determining the site(s) of modification by an irreversible inhibitor is liquid chromatography tandem MS (LC-MS/MS) of peptides that derive from trypsin-mediated cleavage of a compound-treated protein. Unfortunately, in the case of SHP2, the lysine- and arginine-rich region surrounding position 279 (Figure S7) precludes the use of trypsin in generating sizable peptides that include C279, and our attempts to use other proteases to cleave **99**-treated Y279C SHP2 CD for LC-MS/MS analysis did not yield definitive results.

We therefore turned to LC-MS analysis of intact **99**-treated SHP2 CD constructs to determine if the compound engages the enzyme irreversibly and in a manner that is dependent on the presence of C279. When we treated Y279C SHP2 CD (100 μM) with slightly more than 1 equiv of **99** (120 μM), we found that the major peak in the MS spectrum was shifted by m/z 377.3 (Figure S9A,B), consistent with a single covalent labeling event, followed by hydrolysis of **99**'s ethyl ester. The presumptive ester hydrolysis may be induced by the formic acid that is present in the mobile phase of the LC-MS experiment, or it is possible that the **99**'s protein binding site serves as an "accidental esterase" and promotes hydrolysis of the compound. A minor peak, consistent with double labeling, is also visible in the spectrum (Figure S9B). It is interesting to note that the minor, off-target labeling of SHP2 by **99** gives rise to a noticeably smaller m/z shift (372.3) than the on-target labeling of C279 (377.3). We have previously found that surface-exposed cysteine residues on the SHP2 catalytic domain (C259, C318, and C486) can be labeled after prolonged exposures to electrophiles,[47] and we hypothesize that the minor, doubly labeled peak derives from a small amount of labeling at one of these cysteines in addition to labeling at C279. Given that the off-target peak shift is also smaller than the molecular weight of **99** (404.4 g/mol), it is likely that hydrolysis of **99**'s ethyl ester is induced generally by formic acid in the LC-MS experiments and is not specific for a protein site.

Wild-type SHP2 CD, which lacks a cysteine at position 279, yielded LC-MS results that corroborated those acquired with the mutant (Figure S9C,D). We found that a large majority of wild-type SHP2 CD remained unlabeled after incubation with **99** (Figure S9D). A minor peak corresponding to singly labeled protein was also observed (peak shift of m/z 373.9), presumably to a small degree of off-target labeling comparable to that observed with Y279C SHP2 CD. No doubly labeled

https://dx.doi.org/10.1021/acs.biochem.0c00471
Biochemistry 2020, 59, 3498−3507

product was detectable in the wild-type SHP2 CD spectrum. In summary, the LC-MS results on both Y279C and wild-type SHP2 CD support a conclusion that C279 is the major target of **99** and that the compound electrophilically engages the nucleophilic C279 side chain. Our LC-MS experiments do not shed light on which of the two potentially electrophilic carbons in **99**'s mixed fumarate ester/amide (β to the ester or β to the amide) is attacked by C279. However, previous work on mixed fumarate ester/amide warheads suggests that the position β to the ester is the functional group's more electrophilic site, and we therefore we hypothesize that the carbon β to the ester is the atom likely to be engaged by C279.[34,48]

Compound 99-Mediated Inhibition in Cell Lysates. This study's previous demonstrations of Y279C-specific SHP2 inhibition by **99** were carried out with purified enzymes. To be potentially useful in cellular models of NSML, however, a Y279C SHP2-specific ligand must be capable of targeting the mutant in the context of a complex cellular proteome. To assess **99**-mediated inhibition in a proteomic mixture, varying concentrations of **99** were incubated with clarified lysates of Y279C and wild-type SHP2 CD-expressing *E. coli* cells, and the relative phosphatase activities of these incubations were measured. We found, in good agreement with previous results of purified enzymes, that **99**-mediated inhibition of Y279C SHP2 CD in a lysate is dose-dependent and specific to the Y279C mutant (Figure 6), albeit with somewhat attenuated

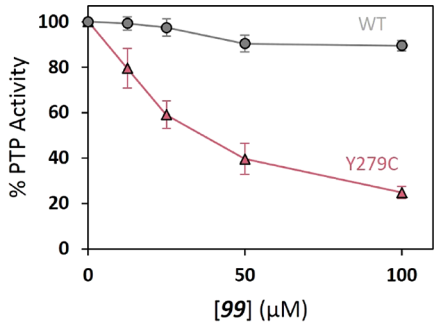

Figure 6. Compound **99** inhibits Y279C SHP2 in a complex proteomic mixture. Clarified lysates (normalized to 1.175 mg/mL total protein) from *E. coli* expressing wild-type (gray circles) or Y279C (pink triangles) SHP2 CD were incubated with the indicated concentrations of **99** for 1 h at 37 °C and then assayed for PTP activity with *p*NPP (wild type) or DiFMUP (Y279C).

potency ($IC_{50} \approx 35\ \mu M$). These data show that **99** is capable of targeting Y279C SHP2 activity, even in the presence of many competing off-target proteins. It is likely, however, that **99**'s modest potency of inhibition may limit its ability to target Y279C SHP2 in cellular or animal models of NSML. Improvement of **99**'s inhibitory properties will likely require future studies that entail more expansive screens of cysteine-reactive compound libraries or that explore and optimize the inhibitor's structure–activity relationships through medicinal chemistry. It is also important to note that the PTP inhibition experiments in lysates do not exclude the possibility that **99** could react with and inhibit with other families of cysteine-dependent enzymes, whose activities are not assessed in the PTP-specific assay.

CONCLUSION

Small molecules that can specifically target pathogenic mutants of signaling proteins potentially represent useful tools for probing and fixing aberrant signaling pathways that are implicated in human disease. In this study, we have described the discovery of **99**, the first known specific inhibitor of Y279C SHP2, which is a causative agent of the developmental disorder NSML. Inhibition of Y279C SHP2 by **99** is dose-dependent, time-dependent, and substrate-independent and is highly specific to Y279C SHP2 over wild-type SHP2, as well as other human PTPs. At the molecular level, our data demonstrate that Y279C SHP2's pathogenic cysteine residue is the molecular target of **99** and that covalent, irreversible engagement of C279 is the key determinant for Y279C-specific SHP2 inhibition. Collectively, these results show that Y279C SHP2 is a viable molecular target for directed pharmaceutical strategies and thus establish a novel approach for the development of anti-NSML therapeutics.

ASSOCIATED CONTENT

Supporting Information

The Supporting Information is available free of charge at https://pubs.acs.org/doi/10.1021/acs.biochem.0c00471.

Figures S1–S9 (PDF)

Accession Codes

Human SHP2, UniProtKB Q06124; human HePTP, UniProtKB P35236; human STEP, UniProtKB P54829; human PTPRR, UniProtKB Q15256; human SHP1, UniProtKB P29350; human PTP1B, UniProtKB P18031; human DEP1, UniProtKB Q12913; human MEG2, UniProtKB P43378; human PTPκ, UniProtKB Q15262.

AUTHOR INFORMATION

Corresponding Author

Anthony C. Bishop – *Department of Chemistry, Amherst College, Amherst, Massachusetts 01002, United States;* orcid.org/0000-0001-8394-280X; Email: acbishop@amherst.edu

Authors

Jenny Y. Kim – *Department of Chemistry, Amherst College, Amherst, Massachusetts 01002, United States*

Bailey A. Plaman – *Department of Chemistry, Amherst College, Amherst, Massachusetts 01002, United States*

Complete contact information is available at: https://pubs.acs.org/10.1021/acs.biochem.0c00471

Author Contributions

J.Y.K. and B.A.P. contributed equally. Experiments were performed by J.Y.K. and B.A.P. Experiments were conceived by A.C.B. in collaboration with J.Y.K. and B.A.P. The manuscript was written by A.C.B. and B.A.P., and all authors have given approval to the final version of the manuscript.

Funding

Research reported in this publication was supported by the National Institute of General Medical Sciences of the National Institutes of Health under Grant R15GM071388 to A.C.B. and by The Arnold and Mabel Beckman Foundation (Beckman Scholars Program) (to J.Y.K. and A.C.B.).

Notes

The authors declare no competing financial interest.

■ ACKNOWLEDGMENTS

Mass spectral data were obtained at the University of Massachusetts Amherst Mass Spectrometry Center. The authors thank Prof. Alberto Lopez for assistance with the acquisition and analysis of NMR data, Chae Young (Clara) Seo for assistance with compound screening, and Prof. Joohyun Lee for use of his lab's RT-PCR machine.

■ REFERENCES

(1) Singh, J., Petter, R. C., Baillie, T. A., and Whitty, A. (2011) The resurgence of covalent drugs. *Nat. Rev. Drug Discovery 10*, 307−317.
(2) Zhang, T., Hatcher, J. M., Teng, M. X., Gray, N. S., and Kostic, M. (2019) Recent advances in selective and irreversible covalent ligand development and validation. *Cell Chem. Biol. 26*, 1486−1500.
(3) Backus, K. M., Correia, B. E., Lum, K. M., Forli, S., Horning, B. D., González-Páez, G. E., Chatterjee, S., Lanning, B. R., Teijaro, J. R., Olson, A. J., Wolan, D. W., and Cravatt, B. F. (2016) Proteome-wide covalent ligand discovery in native biological systems. *Nature 534*, 570−574.
(4) Hallenbeck, K. K., Turner, D. M., Renslo, A. R., and Arkin, M. R. (2016) Targeting non-catalytic cysteine residues through structure-guided drug discovery. *Curr. Top. Med. Chem. 17*, 4−15.
(5) Abdeldayem, A., Raouf, Y. S., Constantinescu, S. N., Moriggl, R., and Gunning, P. T. (2020) Advances in covalent kinase inhibitors. *Chem. Soc. Rev. 49*, 2617−2687.
(6) Chaikuad, A., Koch, P., Laufer, S. A., and Knapp, S. (2018) The cysteinome of protein kinases as a target in drug development. *Angew. Chem., Int. Ed. 57*, 4372−4385.
(7) Visscher, M., Arkin, M. R., and Dansen, T. B. (2016) Covalent targeting of acquired cysteines in cancer. *Curr. Opin. Chem. Biol. 30*, 61−67.
(8) Ostrem, J. M., Peters, U., Sos, M. L., Wells, J. A., and Shokat, K. M. (2013) K-Ras(G12C) inhibitors allosterically control GTP affinity and effector interactions. *Nature 503*, 548−551.
(9) Canon, J., Rex, K., Saiki, A. Y., Mohr, C., Cooke, K., Bagal, D., Gaida, K., Holt, T., Knutson, C. G., Koppada, N., Lanman, B. A., Werner, J., Rapaport, A. S., San Miguel, T., Ortiz, R., Osgood, T., Sun, J. R., Zhu, X. C., McCarter, J. D., Volak, L. P., Houk, B. E., Fakih, M. G., O'Neil, B. H., Price, T. J., Falchook, G. S., Desai, J., Kuo, J., Govindan, R., Hong, D. S., Ouyang, W. J., Henary, H., Arvedson, T., Cee, V. J., and Lipford, J. R. (2019) The clinical KRAS(G12C) inhibitor AMG 510 drives anti-tumour immunity. *Nature 575*, 217−223.
(10) Lanman, B. A., Allen, J. R., Allen, J. G., Amegadzie, A. K., Ashton, K. S., Booker, S. K., Chen, J. J., Chen, N., Frohn, M. J., Goodman, G., Kopecky, D. J., Liu, L., Lopez, P., Low, J. D., Ma, V., Minatti, A. E., Nguyen, T. T., Nishimura, N., Pickrell, A. J., Reed, A. B., Shin, Y., Siegmund, A. C., Tamayo, N. A., Tegley, C. M., Walton, M. C., Wang, H. L., Wurz, R. P., Xue, M., Yang, K. C., Achanta, P., Bartberger, M. D., Canon, J., Hollis, L. S., McCarter, J. D., Mohr, C., Rex, K., Saiki, A. Y., San Miguel, T., Volak, L. P., Wang, K. H., Whittington, D. A., Zech, S. G., Lipford, J. R., and Cee, V. J. (2020) Discovery of a covalent inhibitor of KRAS(G12C) (AMG 510) for the treatment of solid tumors. *J. Med. Chem. 63*, 52−65.
(11) Tartaglia, M., Martinelli, S., Stella, L., Bocchinfuso, G., Flex, E., Cordeddu, V., Zampino, G., van der Burgt, I., Palleschi, A., Petrucci, T. C., Sorcini, M., Schoch, C., Foa, R., Emanuel, P. D., and Gelb, B. D. (2006) Diversity and functional consequences of germline and somatic PTPN11 mutations in human disease. *Am. J. Hum. Genet. 78*, 279−290.
(12) Martinelli, S., Nardozza, A. P., Delle Vigne, S., Sabetta, G., Torreri, P., Bocchinfuso, G., Flex, E., Venanzi, S., Palleschi, A., Gelb, B. D., Cesareni, G., Stella, L., Castagnoli, L., and Tartaglia, M. (2012) Counteracting effects operating on Src homology 2 domain-containing protein-tyrosine phosphatase 2 (SHP2) function drive selection of the recurrent Y62D and Y63C substitutions in Noonan syndrome. *J. Biol. Chem. 287*, 27066−27077.
(13) Yu, Z.-H., Xu, J., Walls, C. D., Chen, L., Zhang, S., Zhang, R., Wu, L., Wang, L., Liu, S., and Zhang, Z.-Y. (2013) Structural and mechanistic insights into LEOPARD syndrome-associated SHP2 mutations. *J. Biol. Chem. 288*, 10472−10482.
(14) Tajan, M., de Rocca Serra, A., Valet, P., Edouard, T., and Yart, A. (2015) SHP2 sails from physiology to pathology. *Eur. J. Med. Genet. 58*, 509−525.
(15) Shen, D. D., Chen, W. X., Zhu, J. L., Wu, G. F., Shen, R. P., Xi, M. Y., and Sun, H. P. (2020) Therapeutic potential of targeting SHP2 in human developmental disorders and cancers. *Eur. J. Med. Chem. 190*, 112117.
(16) Liu, Q. Q., Qu, J., Zhao, M. X., Xu, Q., and Sun, Y. (2020) Targeting SHP2 as a promising strategy for cancer immunotherapy. *Pharmacol. Res. 152*, 104595.
(17) Neel, B. G., Gu, H. H., and Pao, L. (2003) The 'Shp'ing news: SH2 domain-containing tyrosine phosphatases in cell signaling. *Trends Biochem. Sci. 28*, 284−293.
(18) Hof, P., Pluskey, S., Dhe-Paganon, S., Eck, M. J., and Shoelson, S. E. (1998) Crystal structure of the tyrosine phosphatase SHP-2. *Cell 92*, 441−450.
(19) Lee, C. H., Kominos, D., Jacques, S., Margolis, B., Schlessinger, J., Shoelson, S. E., and Kuriyan, J. (1994) Crystal structures of peptide complexes of the amino-terminal SH2 domain of the Syp tyrosine phosphatase. *Structure 2*, 423−438.
(20) Chen, Y. N. P., LaMarche, M. J., Chan, H. M., Fekkes, P., Garcia-Fortanet, J., Acker, M. G., Antonakos, B., Chen, C. H. T., Chen, Z. L., Cooke, V. G., Dobson, J. R., Deng, Z., Fei, F., Firestone, B., Fodor, M., Fridrich, C., Gao, H., Grunenfelder, D., Hao, H. X., Jacob, J., Ho, S., Hsiao, K., Kang, Z. B., Karki, R., Kato, M., Larrow, J., La Bonte, L. R., Lenoir, F., Liu, G., Liu, S. M., Majumdar, D., Meyer, M. J., Palermo, M., Perez, L., Pu, M. Y., Price, E., Quinn, C., Shakya, S., Shultz, M. D., Slisz, J., Venkatesan, K., Wang, P., Warmuth, M., Williams, S., Yang, G. Z., Yuan, J., Zhang, J. H., Zhu, P., Ramsey, T., Keen, N. J., Sellers, W. R., Stams, T., and Fortin, P. D. (2016) Allosteric inhibition of SHP2 phosphatase inhibits cancers driven by receptor tyrosine kinases. *Nature 535*, 148−152.
(21) Nichols, R. J., Haderk, F., Stahlhut, C., Schulze, C. J., Hemmati, G., Wildes, D., Tzitzilonis, C., Mordec, K., Marquez, A., Romero, J., Hsieh, T., Zaman, A., Olivas, V., McCoach, C., Blakely, C. M., Wang, Z. P., Kiss, G., Koltun, E. S., Gill, A. L., Singh, M., Goldsmith, M. A., Smith, J. A. M., and Bivona, T. G. (2018) RAS nucleotide cycling underlies the SHP2 phosphatase dependence of mutant BRAF-, NF1- and RAS-driven cancers. *Nat. Cell Biol. 20*, 1064−1073.
(22) Huang, W.-Q., Lin, Q., Zhuang, X., Cai, L.-L., Ruan, R.-S., Lu, Z.-X., and Tzeng, C.-M. (2014) Structure, function, and pathogenesis of SHP2 in developmental disorders and tumorigenesis. *Curr. Cancer Drug Targets 14*, 567−588.
(23) Martínez-Quintana, E., and Rodríguez-González, F. (2012) LEOPARD syndrome: Clinical features and gene mutations. *Mol. Syndromol. 3*, 145−157.
(24) Yu, Z.-H., Zhang, R.-Y., Walls, C. D., Chen, L., Zhang, S., Wu, L., Liu, S., and Zhang, Z.-Y. (2014) Molecular basis of gain-of-function LEOPARD syndrome-associated SHP2Mutations. *Biochemistry 53*, 4136−4151.
(25) Qiu, W., Wang, X., Romanov, V., Hutchinson, A., Lin, A., Ruzanov, M., Battaile, K. P., Pai, E. F., Neel, B. G., and Chirgadze, N. Y. (2014) Structural insights into Noonan/LEOPARD syndrome-related mutants of protein-tyrosine phosphatase SHP2 (PTPN11). *BMC Struct. Biol. 14*, 10.
(26) Oishi, K., Zhang, H., Gault, W. J., Wang, C. J., Tan, C. C., Kim, I. K., Ying, H. W., Rahman, T., Pica, N., Tartaglia, M., Mlodzik, M., and Gelb, B. D. (2009) Phosphatase-defective LEOPARD syndrome mutations in PTPN11 gene have gain-of-function effects during Drosophila development. *Hum. Mol. Genet. 18*, 193−201.
(27) Cui, H., Song, L., Zhu, C. S., Zhang, C., Tang, B., Wang, S. W., Wu, G. X., Zou, Y. B., Huang, X. H., Hui, R. T., Wang, S. Y., and Wang, J. Z. (2019) mTOR pathway in human cardiac hypertrophy caused by LEOPARD syndrome: a different role compared with animal models? *Orphanet Journal of Rare Diseases 14*, 252.

https://dx.doi.org/10.1021/acs.biochem.0c00471
Biochemistry 2020, 59, 3498−3507

(28) Marin, T. M., Keith, K., Davies, B., Conner, D. A., Guha, P., Kalaitzidis, D., Wu, X., Lauriol, J., Wang, B., Bauer, M., Bronson, R., Franchini, K. G., Neel, B. G., and Kontaridis, M. I. (2011) Rapamycin reverses hypertrophic cardiomyopathy in a mouse model of LEOPARD syndrome-associated PTPN11 mutation. *J. Clin. Invest. 121*, 1026−1043.
(29) Wang, J. X., Chandrasekhar, V., Abbadessa, G., Yu, Y., Schwartz, B., and Kontaridis, M. I. (2017) In vivo efficacy of the AKT inhibitor ARQ 092 in Noonan Syndrome with multiple lentigines-associated hypertrophic cardiomyopathy. *PLoS One 12*, No. e0178905.
(30) Plaman, B. A., Chan, W. C., and Bishop, A. C. (2019) Chemical activation of divergent protein tyrosine phosphatase domains with cyanine-based biarsenicals. *Sci. Rep. 9*, 16148.
(31) Davis, O. B., and Bishop, A. C. (2012) Specific inhibition of sensitized protein tyrosine phosphatase 1B (PTP1B) with a biarsenical probe. *Bioconjugate Chem. 23*, 272−278.
(32) Chio, C. M., Lim, C. S., and Bishop, A. C. (2015) Targeting a cryptic allosteric site for selective inhibition of the oncogenic protein tyrosine phosphatase Shp2. *Biochemistry 54*, 497−504.
(33) Zhang, Z. Y., Maclean, D., Thieme-Sefler, A. M., Roeske, R. W., and Dixon, J. E. (1993) A continuous spectrophotometric and fluorimetric assay for protein tyrosine phosphatase using phosphotyrosine-containing peptides. *Anal. Biochem. 211*, 7−15.
(34) Zaro, B. W., Whitby, L. R., Lum, K. M., and Cravatt, B. F. (2016) Metabolically labile fumarate esters impart kinetic selectivity to irreversible inhibitors. *J. Am. Chem. Soc. 138*, 15841−15844.
(35) Kathman, S. G., Xu, Z., and Statsyuk, A. V. (2014) A fragment-based method to discover irreversible covalent inhibitors of cysteine proteases. *J. Med. Chem. 57*, 4969−4974.
(36) Cunnick, J. M., Mei, L., Doupnik, C. A., and Wu, J. (2001) Phosphotyrosines 627 and 659 of Gab1 constitute a bisphosphoryl tyrosine-based activation motif (BTAM) conferring binding and activation of SHP2. *J. Biol. Chem. 276*, 24380−24387.
(37) Wright, T. A., Stewart, J. M., Page, R. C., and Konkolewicz, D. (2017) Extraction of thermodynamic parameters of protein unfolding using parallelized differential scanning fluorimetry. *J. Phys. Chem. Lett. 8*, 553−558.
(38) Torosyan, H., and Shoichet, B. K. (2019) Protein stability effects in aggregate-based enzyme inhibition. *J. Med. Chem. 62*, 9593−9599.
(39) McGovern, S. L., Helfand, B. T., Feng, B., and Shoichet, B. K. (2003) A specific mechanism of nonspecific inhibition. *J. Med. Chem. 46*, 4265−4272.
(40) Feng, B. Y., and Shoichet, B. K. (2006) A detergent-based assay for the detection of promiscuous inhibitors. *Nat. Protoc. 1*, 550−553.
(41) Blaskovich, M. A. (2009) Drug discovery and protein tyrosine phosphatases. *Curr. Med. Chem. 16*, 2095−2176.
(42) He, R.-j., Yu, Z.-h., Zhang, R.-y., and Zhang, Z.-y. (2014) Protein tyrosine phosphatases as potential therapeutic targets. *Acta Pharmacol. Sin. 35*, 1227−1246.
(43) Andersen, J. N., Mortensen, O. H., Peters, G. H., Drake, P. G., Iversen, L. F., Olsen, O. H., Jansen, P. G., Andersen, H. S., Tonks, N. K., and Møller, N. P. (2001) Structural and evolutionary relationships among protein tyrosine phosphatase domains. *Mol. Cell. Biol. 21*, 7117−7136.
(44) Sarmiento, M., Puius, Y. A., Vetter, S. W., Keng, Y. F., Wu, L., Zhao, Y., Lawrence, D. S., Almo, S. C., and Zhang, Z. Y. (2000) Structural basis of plasticity in protein tyrosine phosphatase 1B substrate recognition. *Biochemistry 39*, 8171−8179.
(45) Parsons, Z. D., and Gates, K. S. (2013) Redox regulation of protein tyrosine phosphatases: methods for kinetic analysis of covalent enzyme inactivation. *Methods Enzymol. 528*, 129−154.
(46) Liu, S. J., Zhou, B., Yang, H. Y., He, Y. T., Jiang, Z. X., Kumar, S., Wu, L., and Zhang, Z. Y. (2008) Aryl vinyl sulfonates and sulfones as active site-directed and mechanism-based probes for protein tyrosine phosphatases. *J. Am. Chem. Soc. 130*, 8251−8260.
(47) Marsh-Armstrong, B., Fajnzylber, J. M., Korntner, S., Plaman, B. A., and Bishop, A. C. (2018) The allosteric site on SHP2's protein tyrosine phosphatase domain is targetable with druglike small molecules. *ACS Omega 3*, 15763−15770.
(48) Tuley, A., and Fast, W. (2018) The taxonomy of covalent inhibitors. *Biochemistry 57*, 3326−3337.

https://dx.doi.org/10.1021/acs.biochem.0c00471
Biochemistry 2020, 59, 3498−3507